Test of active personal dosimeters for interventional radiology in realistic radiation fields

L. Struelens[a*], J. Daures[b], J.-M. Bordy[b], I. Clairand[c], J. Debroas[c], M. Denozières[b], L. Donadille[c], F. d'Errico[d] and C. Itié[c]

[a]Belgian Nuclear Research Centre SCK•CEN, Belgium
[b]French Atomic Energy Commission CEA,LIST, Laboratoire National Henri Becquerel, Gif sur Yvette, 91191, France
[c]Institut de Radioprotection et de Sûreté Nucléaire, BP 17, 92262 Fontenay-aux-Roses Cedex, France
[d]Università degli Studi di Pisa, Italy and Yale University, USA

Abstract. In Interventional radiology, the medical staff stands close to the patient during his exposure to X-rays. Consequently, they can be exposed to relatively high doses due to radiation scattered by the patient and the medical equipment. Contrary to the passive dosemeters which assess the doses a posteriori, APDs are able to warn the medical staff when doses and/or dose rates exceed pre-defined radiation protection limits. At interventional radiology workplaces, APDs must be able to measure low-energy photons (10-120 keV) and pulsed radiations with relatively high instantaneous dose rates delivered by medical X-rays generators. Six ADP models, considered as suitable for application in interventional radiology on the basis of the results of a previous comparison jointly organised by EURADOS and IAEA, were selected to carry out a new comparison in 2007. This included radiation fields able to mimic the scattered and pulsed X-ray radiation fields met at workplace in hospitals. Irradiations took place at CEA-LIST LNHB (Saclay, France) and IRSN (Fontenay-aux-Roses, France). This paper describes the irradiation assemblies both for realistic and classic calibration facilities. The reference values of the personal dose equivalent, $H_p(10)$, were determined through measurements and simulations to calculate the response of the APDs. The results shed light on the ability of APDs to measure correctly the doses, when used in the specific low-energy spectra and dose rates of pulsed X-rays encountered in interventional radiology.

KEYWORDS: active personal dosemeters; intercomparison; interventional radiology; X-rays.

1. Introduction

The evaluation of active personal dosemeters (APDs) in interventional radiology was performed by work package 7 (Radiation protection dosimetry of medical staff) of the CONRAD project, which is a Coordination Action supported by the European Commission within its 6th Framework Program. The objective of WP7 was to promote and co-ordinate research activities for the assessment of occupational exposure to staff at workplaces in therapeutic and diagnostic radiology and nuclear medicine.

APDs are used for the monitoring of occupational doses in many applications of ionising radiation. In interventional radiology, the possibility to assess the dose in real time is particularly interesting since operators are liable to receive relatively high doses while standing close to the primary radiation field and being exposed to radiation scattered by the patient. For the adequate dosimetry of these scattered photons, APDs should be able to measure low-energy (10-120 keV) and pulsed radiation with relatively high instantaneous dose rates. Unfortunately, the current APDs are not always adequate. This problem was clearly highlighted during an international intercomparison organised by EURADOS and IAEA [1].
An evaluation of the behaviour of six APD models that, according to the manufacturers and the IAEA (2007) results, were considered suitable for application in interventional radiology was performed through an intercomparison. Its aim was the identification of the APDs which provide a correct response when used in the specific low-energy spectra and dose rates of pulsed X-rays encountered in

[*] Presenting author, E-mail: lara.struelens@sckcen.be

interventional radiology. The results of this intercomparison are not the scope of this paper, they can be found in *Clairand, et al., 2008* [2].

This paper describes the irradiation assemblies that were set up both for realistic and classic calibration facilities. It focuses on the reference values of the personal dose equivalent, $H_p(10)$, which were determined through measurements and simulations in order to be able to calculate the response of the different APDs.

2. Materials and method

2.1 Design of a realistic calibration field for interventional radiology

In interventional radiology the X-ray tube is most of the time located under the patient and the radiologist stands at his side, often at the level of the hip. Thus, the doctor is exposed to the radiation scattered by the patient. Sometimes, collective protection equipments (e.g. screens, table curtains) are available and can be used to partly reduce the dose received by the doctor. The image intensifier is located symmetrically to the X-ray tube with respect to the patient (see figure 1).

The idea was to propose an irradiation assembly which could be set up easily in any primary or secondary calibration laboratory. From a real workplace situation few simplifications were introduced. First, as it was found that the image intensifier and the patient table do not contribute significantly to the scattered radiation field at the doctor's level, they were not included, however the attenuation of the table was included in the total filtration considered. Secondly, the patient was replaced by an ISO water slab phantom [3]. The surgeon was represented by an ISO slab phantom on which the dosemeters were irradiated. On figure 2 the irradiation configuration is shown. It can be seen that the doctor-phantom was shifted from the level of the hip of the patient to the side face of the patient-phantom. Calculations showed that the energy distributions at both locations are similar but the total fluence is multiplied by a factor of 3.6 when moving the calibration point. Detailed results on the design of the calibration field can be found in *Bordy et al., 2008* [4].

2.2 Description of the facilities and intercomparison configuration

The intercomparison of the APDs was performed with pulsed and continuous X-ray beams, available respectively at the Laboratoire National Henri Becquerel (LNHB) at CEA-LIST, the French National Metrology Laboratory for ionizing radiation in Saclay, and at a metrology laboratory of the Institute of Radiological Protection and Nuclear Safety (IRSN) in Fontenay-aux-Roses. Both laboratories are accredited according to the ISO standard 17025 [5]. The diagnostic pulsed X-ray beam was generated with a MPH65 (GEMS) medical X-ray unit designed to generate only one pulse at a time. The continuous X-ray beam was generated with a 100 kV (Philips) X-ray unit.

A configuration close to clinical practice was considered: peak tube voltage and filtration of 70 kVp and (4.5 mm Al + 0.2 mm Cu), respectively. Because collimation devices did not have the same geometry (circular and square for continuous and pulsed facilities, respectively), the collimator openings were chosen such as the areas of both (non-scattered) beam cross sections were the same (around 290 cm² at 95 cm from the source). The distances between the different equipment and the phantoms were taken from information gathered from the practitioners.

Figure 1: Side and top views of the workplace configuration.

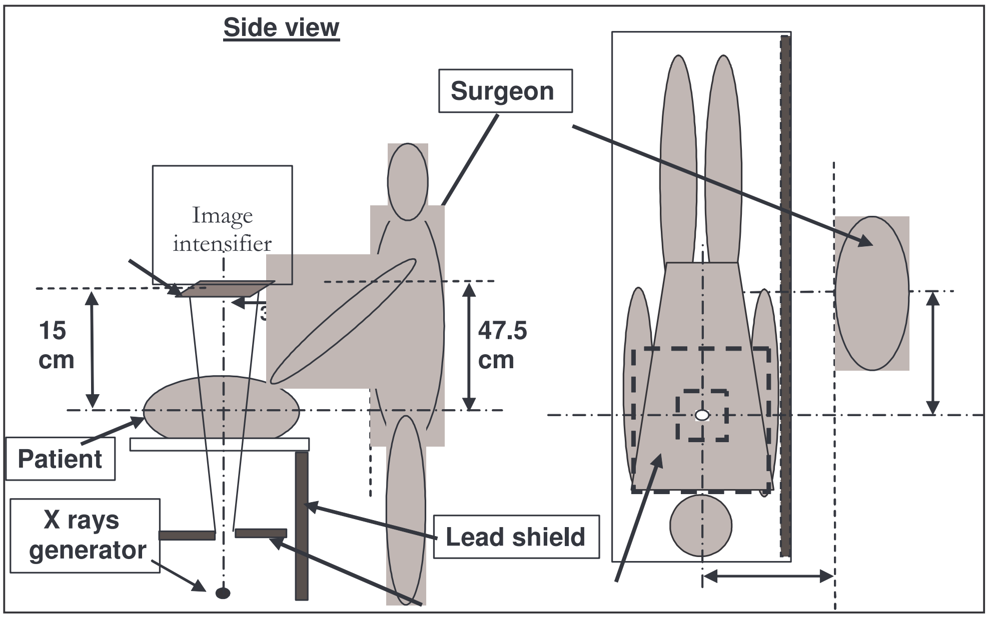

Figure 2: Side and top view of the simplified configuration used for the intercomparison.

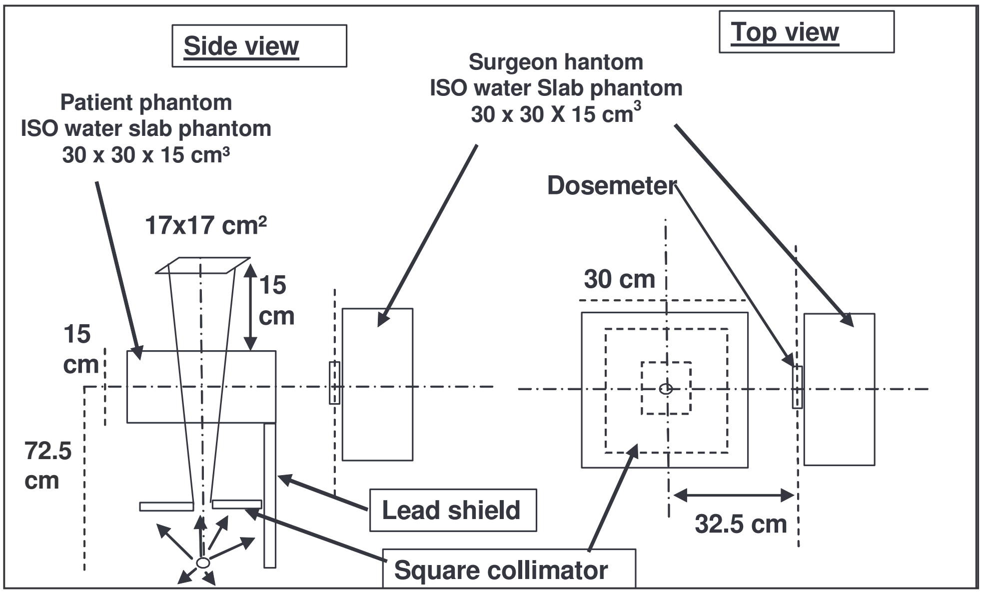

For the pulsed facility, a pulse width of 100 ms was used. It has to be noticed that clinical pulse widths can vary within few ms to few hundreds ms depending on the examination, X-ray installation and practice. The patient phantom's front wall was positioned at 65 cm from the source. APDs were irradiated one by one at the centre of the radiologist phantom's front wall. The centre of the radiologist phantom was positioned at the same level as the centre of the patient phantom (72.5 cm from the source). The centre of the tested APD was shifted by 32.5 cm in the normal direction with respect to the beam axis. A lead shield was used to remove the X-ray component produced through scattering in the tube housing and irradiating the radiologist phantom (and the dosemeter). Without the shield, this scatter component appeared to increase the dose rate by more than 30% at the dosemeter position and it was shown that it was due to scattering in the filters.

2.3 Reference quantities

It was necessary to determine a reference value in terms of $H_p(10)$ in the scattered beam at the position of the APD. First, free in air kerma K_a was measured with a calibrated cavity chamber at the point of test in the scattered beam. At this point, K_a rates were found equal to 3.03 mGy.h^{-1} and 3.20 µGy.pulse^{-1} for the continuous and pulsed installations, respectively. The overall uncertainties on K_a were estimated to 1.2 % and 1.0 % (k = 1) for the continuous and pulsed installations, respectively. Next, a conversion coefficient was needed to convert air kerma into $H_p(10)$. The published conversion coefficients from K_a to $H_p(10)$ [6] are defined for parallel, expanded radiation fields, which are not representative for the considered energy and angular distributions in the scattered field used for this intercomparison. Thus, Monte Carlo calculations were performed for the determination of $H_p(10)/K_a$ for the specific scattered beam spectrum. Different codes were used: MCNP4C [7], MCNP5 [8], MCNPX [9] and Penelope 2006 [10].

K_a was calculated in a 1 cm radius sphere filled with air centered at the test point, in the absence of the radiologist phantom. $H_p(10)$ was calculated as the dose absorbed in a cell centered at the test point and positioned at 10 mm within the 30x30x15 cm³ ICRU slab phantom. The lead shield was introduced as well in the model, with 65 cm height and covering the whole patient phantom width (30 cm).

The source filtered 70 kVp X-ray spectrum used in the Monte Carlo simulations was calculated with the deterministic software XCOMP-5 [11], taking into account the filtration (4.5 mm Al + 0.2 mm Cu) and the different tungsten anode angles. This means that filters were not explicitly introduced in the simulations. However, the XCOMP-5 filtered spectrum was checked against an MCNPX calculation (figure 3) in which the source unfiltered spectrum (calculated by XCOMP-5) was filtered by 4.5 mm Al and 0.2 mm Cu. It can be seen that the agreement is very good and that the source spectrum ranges from around 25 keV up to 70 keV. From this comparison it was also observed that less than 10% of the collimated source flux is transmitted through the filters. From the source, considered as a point-like isotropic X-ray emitter, collimation was taken into account by restricting the emission angles to a cone with appropriate opening solid angle. In the instance of the pulsed installation, for which the collimator was a square, an additional perfect square collimator (null importance for photons) was defined. All tricks previously mentioned (not explicitly defining filters and collimators), although strongly simplifying reality, allowed to greatly speed-up calculations.

Only photons were transported (kerma approximation: secondary electrons generated by photon interaction deposit their energy locally), detailed photon physics treatment, as defined in MCNP4C manual, was considered and all photon physical processes taking place at these energies, i.e. fluorescence emission, photoelectric absorption, incoherent (Compton) and coherent (Thomson) scattering, were taken into account.

Absorbed dose was calculated by different techniques, either by fluence tallies (F2, F4, F5 in MCNP) multiplied by appropriate ICRU conversion coefficients, or dose tally (F6 in MCNP), or energy deposition tally (*F8 in MCNP). For the fluence tallies, the dosimetric quantities (either K_a or $H_p(10)$, as appropriate) were calculated by folding the fluence with the conversion coefficient taken from ICRU report 57 [5] according to the following equations:

$$K_a = \int_E \phi_E \left[\frac{K_a}{\phi}\right](E)\, dE \qquad\qquad H_p(10) = \int_E \phi_E \left[\frac{H_{p,slab}(10,0°)}{\phi}\right](E)\, dE$$

where the ratios K_a/ϕ and $H_{p,slab}(10,0°)/\phi$ are the appropriate conversion coefficients.

To determine the reference $H_p(10)_{ref}$ value, $H_p(10)/K_a$ calculated as previously explained was multiplied by the measured reference value in terms of air kerma $K_{a,ref}$

$$H_p(10)_{ref} = {}^{H_p(10)}\!/_{K_{air}} \times K_{air,ref}$$

For the continuous beam, the reference K_a at the test point was 150 µGy after 178 s of irradiation and for the pulsed beam, the reference K_a at the test point was 80 µGy after 25 pulses.

Figure 3: Unfiltered and filtered by 4.5 mm Al and 0.2 mm Cu 70 kVp X-ray spectra, on an arbitrary unit, calculated with XCOMP-5 [10] for a tungsten anode with angle 20°;
the filtered spectrum is compared to an MCNPX calculation with an unfiltered source spectrum, filtered by 4.5 mm Al and 0.2 mm Cu.

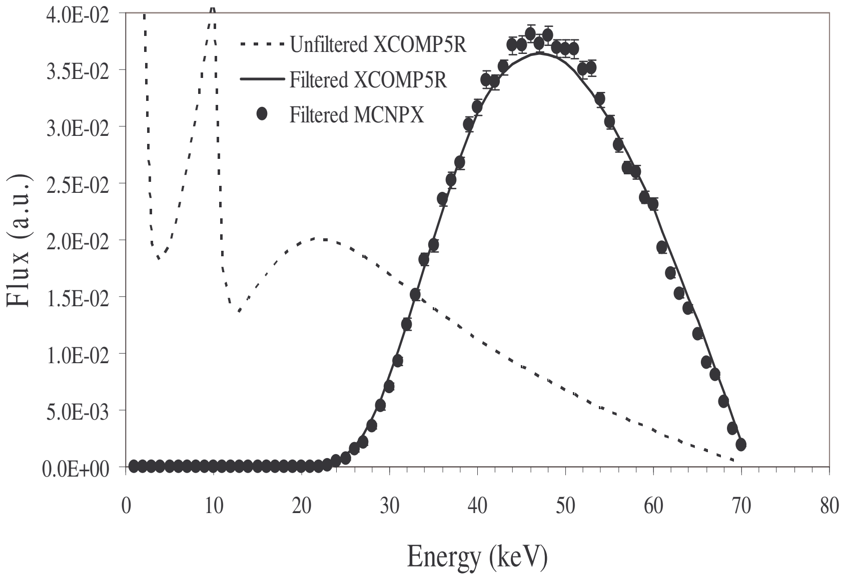

3. Results

Three different laboratories performed calculations to define the appropriate conversion coefficient from K_a to $H_p(10)$ for the considered energy spectrum in the scattered field: CEA-LIST (LNHB), IRSN and SCK•CEN. In table 1, all calculation results are summarized.

A study on the angular dependence of the scattered radiation was performed, calculating the spectra for different angles with respect to the normal axis of the radiologist-phantom and considering the $H_p(10, \alpha)/H_p(10, 0°)$ coefficients in ICRU Report 57 [6]. We could conclude, however, that this study changed the conversion coefficient $H_p(10)/K_a$ by less than 2%.

The $H_p(10)/K_a$ conversion coefficient that we used for the intercomparison was 1.40 Sv.Gy^{-1}, i.e. a mean value between the estimates from the different codes using dose (tally F6 in MCNP) or energy deposition (tally *F8 in MCNP) tallies. Taking into account both Monte Carlo statistical (type A) errors and scattering of the different results around the mean value, that accounts for type B errors, the uncertainty on the $H_p(10)/K_a$ conversion coefficient could be estimated to 1.2 % (k = 1). However, since all calculation results were obtained with similar and simplified models for the radiation source and the geometry, an additional type B uncertainty on the conversion coefficient was assumed, leading to a total relative uncertainty estimated to 3 % (k = 1).
Thus, the conversion coefficient was taken as:

$$\frac{H_p(10)}{K_{air}} = 1.40\ Sv.Gy^{-1} \pm 3\%$$

4. Discussion

The $H_p(10)/K_a$ conversion coefficient that we used for this intercomparison was 1.40 $Sv.Gy^{-1}$, i.e. a mean value between the estimates from the different codes using dose (tally F6 in MCNP) or energy deposition (tally *F8 in MCNP) tallies. It is interesting to notice that if K_a and $H_p(10)$ were calculated through fluence spectrum (tallies F2, F4 or F5 in MCNP) folded with the energy-dependent ICRU report 57 [6] conversion coefficients at 0°, a value around 1.5 $Sv.Gy^{-1}$ was obtained, i.e. 7 % larger than 1.40 $Sv.Gy^{-1}$. This is due to the fact that ICRU hypotheses were not fulfilled for the investigated configuration, i.e. (1) the scattered X-ray beam incident on the radiologist-phantom was not parallel, though angular effects were shown to be small and (2) the radiologist-phantom was not homogeneously (and not completely) irradiated, thus leading to a reduced contribution of backscattered photons. The latter point provides the principal explanation of the different conversion coefficients between the two calculation methods. Therefore, ICRU report 57 conversion coefficients should not be used in combination with the fluence spectra calculated for this study.

Table 1: Summary of all calculation results of $H_p(10)/K_a$ for CEA-LIST, IRSN and SCK•CEN

X 10^{-6} (pGy/history or pSv/history)		K_a			$H_p(10)$			$H_p(10)/K_a$		
		F5	F6	*F8	F5	F6	*F8	F5	F6	*F8
CEA-LIST	MCNP4C - lib02p square field	4.64 (0.2%)	4.40 (0.3%)	4.42 (1.2%)	6.97 (0.2%)	6.31 (0.6%)	6.33 (3.0%)	1.50	1.43	1.43
	MCNP5 - lib04p square field	4.29 (0.2%)	4.38 (0.2%)	4.35 (0.7%)	6.44 (0.2%)	6.23 (0.4%)	6.16 (1.9%)	1.50	1.42	1.42
	Penelope2006 square field		4.87 (2.6%)			6.77 (0.5%)			1.39	
IRSN	MCNPx2.5f - lib04p circular field		4.83 (0.7%)			6.75 (0.5%)			1.40	
	MCNPx2.5f - lib04p square field		4.85 (0.7%)			6.80 (0.6%)			1.40	
SCK•CEN	MCNPx2.5.0 – lib04p square field	4.67 (0.04%)	4.93 (0.7%)	4.93 (1.0%)	7.06 (0.03%)	6.96 (0.6%)	6.91 (0.9%)	1.51	1.41	1.40

As mentioned before, in the experiments an additional lead shield was used to attenuate most of the scattered radiation produced in the filters. These filters are inserted after the collimation system. When calculations are performed with and without this lead shield, the K_a ratio at the test point between both configurations without and with lead shield is close to unity (1.06). However, when K_a at the test point was measured with and without lead shield, a ratio of 1.30 and 1.94 was obtained at the pulsed and continuous installations, respectively. These differences between both experimental facilities and between measurements and calculations led us assume that some of the experimental conditions are not well reproduced in the calculation models. When the filtration is explicitly taken into account in the calculation model, starting from an unfiltered spectrum, filtered in the model by 4.5 mm Al + 0.2 mm Cu (figure 3), a K_a ratio without and with lead shield is found to be 2.45 (for the continuous installation), which is closer to the measurements.

It was also observed that there was a difference in position of the lead shield between both installations, but it was investigated that this factor could not have an impact larger than 5 % on the resulted measurements.

To complete the investigation of the differences between both experimental installations and between experiments and calculations, the sensitivity of the results with respect to the knowledge we have about the X-ray tube has been investigated. These results can be found in more detail in *Struelens et al, 2008* [12].

5. Conclusions

Active personal dosemeters measure dose equivalents and dose equivalent rates in real time and provide adjustable audible alarms. They are efficient tools to help reducing doses by optimising practices as well as collective and individual protection. They are of particular interest in situations with possible high doses and/or dose rates as in the medical field. During interventional procedures the staff is standing close to the primary X-ray radiation field and is exposed to radiation scattered by the patient. In these situations, APDs should accurately respond to low energy (10-120 keV) and pulsed photon fields.

An intercomparison of selected APDs was carried out in continuous and pulsed radiation fields similar to the field characteristics met at interventional medical workplaces. This paper has described the preparatory work for such an intercomparison, such as the design and the implementation of a realistic calibration facility for these kinds of procedures and the calculations necessary to determine the reference dose equivalent value $H_p(10)$.

A conversion coefficient $H_p(10)/K_a$ was calculated of 1.40 $Sv.Gy^{-1}$ ± 3% for the specific scattered radiation field used for the intercomparison.

Differences were observed between measurements in the two experimental laboratories and between measurements and calculations. It was concluded that the observed differences come from the assumptions made about the geometry of the X-ray tubes and that the simulation models of the X-ray tubes might be too simple, particularly when calculations and measurements are performed in the scattered beam. We should also bare in mind, as there is no absolute Monte Carlo computer code, it is normal to find some discrepancies between experiments and calculations. This lay emphasis on the need of accurate calibration of the transfer dosemeters used to measure the dose rate at the point of test.

6. References

[1] INTERNATIONAL ATOMIC ENERGY AGANCY. Intercomparison of Personal Dose Equivalent Measurements by Active Personal Dosemeters. Final Report of a joint IAEA-EURADOS Project. IAEA Report IAEA-TECDOC-1564 (2007)

[2] CLAIRAND, I., et al., Intercomparison of active personal dosemeters in interventional radiology. Radiat. Prot. Dosim (2008). doi:10.1093/rpd/ncn083.

[3] INTERNATIONAL ORGANISATION FOR STANDARDIZATION. X and gamma reference radiation for calibrating dosemeters and doserate meters and for determining their response as a function of photon energy — Part 3: Calibration of area and personal dosemeters and the measurement of their response as a function of energy and angle of incidence. International Standard ISO 4037-3 (1999).

[4] BORDY, J.M., et al., Design of a realistic calibration field for diagnostic radiology (medical staff dosimetry). In Proceedings of the International Workshop on Uncertainty Assessment in Computational Dosimetry, a comparison of approaches, Bologna, Italy, 8-10 October 2008 (in press).

[5] INTERNATIONAL ORGANISATION FOR STANDARDIZATION. General requirements for the competence of testing and calibration laboratories. International Standard ISO 17025 (2005).

[6] INTERNATIONAL COMMISSION ON RADIATION UNITS AND MEASUREMENTS (ICRU). Tissue Substitutes in Radiation Dosimetry and Measurement. ICRU Report 44 (Bethesda, MD: ICRU Publications) (1998).
[7] BREISMEISTER, J.F. (ed.) MCNP^{TM} – A general Monte Carlo N-particle transport code, version 4C, Los Alamos National Laboratory. Report LA-13709-M (2000).
[8] MCNP – A general Monte Carlo N-particle transport code, version 5, Los Alamos National Laboratory. Report LA-UR-03-1987 (2003, revised 2004).
[9] PELOWITZ, D.B. (ed.) MCNPX User's manual, version 2.5.0. Los Alamos National Laboratory. Report LA-CP-05-0369 (2005).
[10] SALVAT, F., FERNANDER-VAREA, J.M., SEMPAU, J., PENELOPE 2006: A Code System for Monte Carlo Simulation of Electron and Photon Transport. Workshop Proceedings Barcelona, Spain 4-7 July 2006, OECD 2006 NEA No. 6222, Nuclear energy agency organisation for economic co-operation and development (2006).
[11] NOWOTNY, R., HOFER, A., XCOMP5, Program for calculating diagnostic x-ray spectra, RoeFo, Fortschr. Geb. Roentgenstr. Nuklearmed. 142, 685-689 (1985).
[12] STRUELENS, L., et al., Monte Carlo modelling for medical staff dosimetry. Summary of the submitted problem solutions. In Proceedings of the International Workshop on Uncertainty Assessment in Computational Dosimetry, a comparison of approaches, Bologna, Italy, 8-10 October 2008 (in press).